ClF was recovered in a quantity indicating that a quantitative conversion had taken place. The isolated product amounted to 94% yield after distillation. The compound is a glass at −85 °C with a vapor pressure of 0.5–1 Torr at 22 °C. IR (neat liquid, KBr windows): 1635 w, 1300 s, 1215 vs, 1125 vs, 1056 s, 990 m, 902 m, 863 m, 818 m, 777 w, 742 w, 724 s, 696 s, 669 w, 647 m, 613 m, 597 w, 540 m, 515 w cm^{-1}. ^{19}F NMR: ϕ −58.24 (t-t), CF_3; ϕ −80.59 (m), CF_2. Major peaks in the mass spectrum, *m/e*: 341, $C_6F_9N_2Cl_2^+$; 287, $C_6F_8N_2Cl^+$; 268, $C_6F_7N_2Cl^+$; 262, $C_6F_{10}^+$; 243, $C_6F_9^+$; 212, $C_5F_8^+$; 193, $C_5F_7^+$; 145, $C_5F_3N_2^+$; 69, CF_3^+.

Preparation of CF_3NCl_2. Into a dry 300-mL Monel Hoke vessel were placed 25 g of CsF and three steel balls. The vessel was evacuated and cooled to −196 °C. Next, 50 mmol of ClCN was condensed into the bomb, followed by 155 mmol of ClF. The system was warmed directly to 22 °C and, with intermittent shaking, was allowed to stand for 6–12 h. At the end of this time, the only detectable volatile compound at 50 Torr by IR analysis was CF_3NCl_2. By repeated separation through traps at −125, −100, and −78 °C, pure CF_3NCl_2 was collected as a liquid in the trap at −78 °C. Only Cl_2 passed through −100 °C and was discarded. The trap at −100 °C contained mostly CF_3NCl_2 with some dissolved Cl_2. The material in this trap was repeatedly run through the system until all of the chlorine was separated from the CF_3NCl_2. In this way, 48 mmol of CF_3NCl_2 was collected. The compound was identified by its IR spectrum. The stoichiometry of the reaction obeys the chemical equation $ClCN + 3ClF \xrightarrow{CsF} CF_3NCl_2 + Cl_2$. The role of CsF appears to be catalytic, since all ClF is consumed in the reaction. Furthermore, a single 10-g charge of CsF was used for 35-, 50-, and 60-mmol batches in succession with no loss of activity or yield.

Thermal Decomposition of $(CF_3)_2C{=}C(CF_2NCl_2)_2$. This thermal decomposition reaction was the only case in which a pure diazene derivative resulted via loss of Cl_2. Typically, 1.58 g (3.66 mmol) $(CF_3)_2C{=}C(CF_2NCl_2)_2$ was injected into a Pyrex tube reactor, which was quickly evacuated and flame-sealed. The system was placed in an oven at 90 °C, and the temperature was then set at 120 °C. Upon this further warming, the chlorine was readily evident, and heating was continued until no more of the dense starting material was seen to reflux on the walls of the tube. When the reaction was over, the tube was connected to the vacuum line, frozen to −196 °C, and cracked open. There were no noncondensable materials at −196 °C, which indicates that dinitrogen was not formed. All the volatile materials were condensed onto Hg, and the amount of Cl_2 taken up was measured. The Cl_2 (6.91 mmol) eliminated corresponded to a 94.4% conversion to a diazene that was subsequently identified by its IR, NMR, and mass spectra and elemental analysis. IR (vapor): 1705 m, 1590 m, 1352 m, 1280–1200 vs, 1116 s, 1058 vs, 1018 m, 955 w, 908 s, 851 s, 827 w, 770 w, 748 s, 710 s, 682 m, 625 s, 547 w, 468 s, 426 m cm^{-1}. ^{19}F NMR: ϕ −61.27 m, CF_3; ϕ −80.69 m, CF_2. Anal. Calcd for $C_6F_{10}N_2$: C, 24.85; F, 65.50; N, 9.66. Found: C, 24.75; F, 65.60; N, 9.73. Major peaks in the mass spectrum, *m/e*: 262, $M^+ - N_2$ ($C_6F_{10}^+$); 243, $C_6F_9^+$; 212, $C_5F_8^+$; 193, $C_5F_7^+$; 143, $C_4F_5^+$; 69, CF_3^+.

Reaction of $KC(CN)_3$ with ClF. In a 150-mL stainless steel Hoke bomb, 0.47 g (3.64 mmol) of previously dried $KC(CN)_3$ was mixed with ~3 mL of dry CCl_3F. The contents were frozen to −196 °C, and an 8:1 mole ratio of ClF was condensed inside. After the contents were warmed from −116 to +22 °C over 12 h, excess ClF and CCl_3F were removed, leaving a nonvolatile dense liquid. During the extraction with pentane, the insoluble KF byproduct was evident. A yield of 90% or higher was obtained under optimum conditions. In cases where $KC(CN)_3$ was not predried or the reaction was scaled to greater than 0.65 g of $KC(CN)_3$, complete degradation of the contents was observed (N_2, CF_4, CF_3Cl). This occurred even when the reactor was allowed to warm slowly from −116 °C. Also, the product must be isolated shortly after the reactor reaches 22 °C or partial decomposition occurs. The impurities that result in this case attack the glass distillation vessel. The pure product was tentatively identified on the basis of its IR and NMR spectra and elemental analysis. The elemental analysis indicated an empirical formula of $C_4Cl_5F_4N_3$. Anal. Calcd for $C_4Cl_5F_4N_3$: Cl, 51.63; F, 22.13; N, 12.24. Found: Cl, 51.17; F, 22.60; N, 12.05. A complex, but symmetric, pattern of 22 resolvable lines was observed in the ^{19}F NMR spectrum centered at ϕ −86.76. No combination of *J* values corresponded to a quartet, indicating that only doublets and triplets comprised the pattern. IR (liquid, NaCl windows): 1633 m, 1238 vs, 1200–1090 vs, 1065 s, 1041 m, 995 m, 965 m, 922, 898 s, 827 s, 735 s, 715 s, 694 s, 631 s, 596 s cm^{-1}.

Conclusion

Our investigation has shown that certain nonfluorinated cyano compounds can now be reacted cleanly with ClF on a relatively large scale. It is likely that the reaction could be applied to many other polycyano compounds, including aromatics. These new *N,N*-dichloro compounds, despite their general resistance to being easily converted to azo derivatives, still show promise as starting materials for further reactions. Work continues in the development of these compounds with respect to their syntheses and uses.

Acknowledgment is made to the National Science Foundation (Grant CHE-8100156) and the Air Force Office of Scientific Research (Grant 82-0247) for financial support.

Contribution from the Departament de Química Inorgànica, Facultat de Química de la Universitat de València, 46100 Burjassot (València), Spain, Dipartimento di Chimica, Università della Calabria, Arcavacata di Rende, Cosenza, Italy, and Departamento de Física Aplicada, Universidad Politécnica de Valencia, València, Spain

Crystal Structure and Magnetic Properties of $[Fe(pyz)_2(NCS)_2]_n$ (pyz = Pyrazine), a 2D Sheetlike Polymer

José Antonio Real,*[1a] Giovanni De Munno,[1b] M. Carmen Muñoz,[1a,c] and Miguel Julve[1a]

Received October 18, 1990

A lot of work has been devoted to the study of exchange interactions between transition-metal ions through extended bridging groups in the last two decades,[2] the fundamental understanding of the long-range magnetic interactions being one of the main reasons. Pyrazine (1,4-diazine), hereafter noted as pyz, has been one of such multiatom bridges that has been widely used because of its ability to yield one-dimensional linear chains or two-dimensional layer compounds.[3] This ligand coordinates to metal ions in a bis-monodentate fashion through its two nitrogen lone pairs leading to intramolecular metal–metal separations of about 6.7 Å.[3b] Thorough discussions of the exchange pathway for pyrazine-containing copper(II) complexes have been carried out in the light of the structural data revealing that an effective d(metal)–π(pyz) overlap is operative in some cases.[3b,c,4,5] In a theoretical paper about orbital interactions in dinuclear complexes[6] the extended Hückel molecular orbital approach was used to predict that pyz would be a very effective ligand to transmit exchange interactions through a σ-type exchange pathway. In general, the interaction through this ligand is weak, and this discrepancy with the theoretical prediction is attributed to the fact that these calculations overemphasize the intermolecular overlap.[5e,6]

(1) (a) Universitat de València. (b) Università della Calabria. (c) Universidad Politécnica de Valencia.
(2) Willet, R. D.; Gatteschi, D.; Kahn, O., Eds. *Magneto-Structural Correlations in Exchange Coupled Systems*; Reidel: Dordrecht, Holland, 1985.
(3) (a) Carreck, P. W.; Goldstein, M.; McPartlin, E. M.; Unworth, W. D. *J. Chem. Soc., Chem. Commun.* **1971**, 1634. (b) Santoro, A.; Mighell, A. D.; Reimann, C. W. *Acta Crystallogr., Sect. B: Struct. Crystallogr. Cryst. Chem.* **1970**, *B26*, 979. (c) Darriet, J.; Haddad, M. S.; Duester, E. N.; Hendrickson, D. N. *Inorg. Chem.* **1979**, *18*, 2679.
(4) (a) Belford, R. C. E.; Fenton, D. E.; Truter, M. R. *J. Chem. Soc., Dalton Trans.* **1974**, 17. (b) Morosin, B.; Hughes, R. C.; Soos, Z. G. *Acta Crystallogr, Sect. B* **1975**, *B31*, 762. (c) Haynes, J. S.; Rettig, S. J.; Sams, J. R.; Thompson, R. C.; Trotter, J. *Can. J. Chem.* **1987**, *65*, 420.
(5) (a) Villa, J. F.; Hatfield, W. E. *J. Am. Chem. Soc.* **1971**, *93*, 4081. (b) Inman, G. W.; Hatfield, W. E. *Inorg. Chem.* **1972**, *11*, 3085. (c) Richardson, H. W.; Hatfield, W. E. *J. Am. Chem. Soc.* **1976**, *98*, 835. (d) Richardson, H. W.; Wasson, J. R.; Hatfield, W. E. *Inorg. Chem.* **1977**, *16*, 484. (e) Haddad, M. S.; Hendrickson, D. N.; Canady, J. P.; Drago, R. S.; Biekzsa, D. S. *J. Am. Chem. Soc.* **1979**, *101*, 898. (f) Boyd, P. D. W.; Mitra, S. *Inorg. Chem.* **1980**, *19*, 3547. (g) Julve, M.; Verdaguer, M.; Faus, J.; Tinti, F.; Moratal, J.; Monge, A.; Gutiérrez-Puebla, E. *Inorg. Chem.* **1987**, *26*, 3520.
(6) Hay, P. J.; Thibeault, J. C.; Hoffmann, R. *J. Am. Chem. Soc.* **1975**, *97*, 4884.
(7) See e.g.: Hendrickson, D. N. In ref 2, p 523 ff.

0020-1669/91/1330-2701$02.50/0

Table I. Crystallographic Data for $[Fe(pyz)_2(NCS)_2]_n$

chem formula $C_{10}H_8FeN_6S_2$	fw 332.2
a = 10.184 (2) Å	space group $C2/m$
b = 10.455 (3) Å	λ = 0.71073 Å
c = 7.155 (1) Å	d_{calcd} = 1.651 g cm^{-3}
β = 118.68 (1) deg	μ = 14.2 cm^{-1}
V = 668.4 (3) Å^3	$R(F_o)$ = 0.0286
Z = 2	$R_w(F_o)$ = 0.0303
T = 25 °C	

The magnetic properties of other pyrazine-containing first-row transition-metal ions such as nickel(II),[8] cobalt(II),[3a,9] and iron(II)[10] have been investigated. In the last case, the extreme insolubility of the isolated complexes is at the origin of the lack of X-ray diffraction studies on single crystals, the structural conclusions being based only on spectroscopic evidence. The variety of magnetic properties exhibited by pyrazine-bridged iron(II) complexes makes single-crystal X-ray structural data invaluable to support the corresponding magneto–structural correlations. The use of slow-diffusion techniques allowed us to grow single crystals of the $[Fe(pyz)_2(NCS)_2]_n$ polymeric compound for the first time, and we report here its crystal structure as well as its magnetic properties as a function of the temperature.

Experimental Section

Growth of Single Crystals. Single crystals of the title compound were obtained by the slow-diffusion method, in aqueous solution under an argon atmosphere, using an H-double-tube glass vessel. The starting materials were aqueous solutions of pyrazine on the one hand and iron(II) sulfate heptahydrate and potassium thiocyanate on the other hand. After 3 weeks, brown crystals were collected, washed with water, and dried in an argon stream. Anal. Calcd for $C_{10}H_8FeN_6S_2$: C, 36.16; H, 2.41; N, 25.31; S, 19.28. Found: C, 35.96; H, 2.30; N, 25.15; S, 18.91. Carbon, hydrogen and sulfur were determined by the Servei de Microanàlisi Elemental (CSIC, Barcelona, Spain).

Magnetic Susceptibility Measurements. These measurements were carried out on samples containing small single crystals in the 4.2–300 K temperature range with a SQUID instrument (SHE Corp.) maintained by the Bordeaux University CRPP. Independence of the susceptibility with regard to the applied magnetic field was checked both at low and room temperatures. Mercury tetrakis(thiocyanato)cobaltate(II) was used as a susceptibility standard. The diamagnetism correction was estimated to be -173×10^{-6} cm^3 mol^{-1} from Pascal's constants.[11] The uncertainty on the temperatures is about ±0.1 K for $4 < T < 50$ K and ±1 K for $T > 100$ K.

X-ray Structure Determination. The intensity data were collected at room temperature on a Siemens R3m/V automatic diffractometer with monochromatized Mo Kα radiation. The crystals were shaped as irregular prisms. Information concerning conditions for crystallographic data collection and structure refinement is summarized in Table I. Lattice parameters were obtained from least-squares refinement of the setting angles of 25 reflections in the $15 \le 2\theta \le 30°$ range. A total of 1011 reflections were collected in the range $3 \le 2\theta \le 55°$ by $\omega/2\theta$ scans; 820 of them were unique, and from these, 771 were assumed as observed ($I \ge 3\sigma(I)$). After every 100 reflections 3 were collected as an intensity and orientation control, and they showed no significant intensity decay. Lorentz–polarization corrections, but no absorption and extinction corrections, were applied.

The structure was solved by Patterson methods with the SHELXTL PLUS program[12] and refined by full-matrix least-squares methods, with $\sum w(|F_o| - |F_c|)^2$ being minimized. Non-hydrogen atoms were treated anisotropically, whereas hydrogen atoms were located from a difference synthesis and refined with an overall isotropic temperature factor. The final R and R_w values were 0.0286 and 0.0303, respectively, with $w = [\sigma^2(F_o) + 0.0004|F_o|^2]^{-1}$ and a goodness of fit of 1.86. All calculations were carried out on a micro-Vax II computer, using the SHELXTL and PARST[13] program package. Final fractional coordinates for non-hydrogen atoms are given in Table II, and bond distances and angles are gathered in Table III. Full crystallographic data, anisotropic thermal parameters, and final hydrogen coordinates are listed in Tables S1–S3.[14]

Table II Final Atomic Fractional Coordinates[a] and Equivalent Isotropic Displacement Parameters[b] for Non-Hydrogen Atoms of $[Fe(pyz)_2(NCS)_2]_n$

atom	x/a	y/b	z/c	10^3U_{eq}, Å^2
Fe	0	0	0	21 (1)
S(1)	0.3546 (1)	0	0.7351 (1)	56 (1)
N(1)	0.1560 (1)	0.1540 (1)	0.0067 (2)	27 (1)
N(2)	0.1092 (3)	0	0.3299 (3)	32 (1)
C(1)	0.2108 (3)	0	0.5013 (4)	28 (1)
C(2)	0.2065 (2)	0.3259 (2)	−0.1665 (3)	39 (1)
C(3)	0.1131 (2)	0.2319 (2)	−0.1601 (3)	39 (1)

[a] Estimated standard deviations in the last significant digits are given in parentheses. [b] U values for anisotropically refined atoms are given in the form of the isotropic equivalent thermal parameter $U_{eq} = {}^1/_3(U_{11} + U_{22} + U_{33})$.

Table III. Bond Distances (Å) and Angles (deg) for $[Fe(pyz)_2(NCS)_2]_n$[a]

Distances			
Fe–N(1)	2.246 (2)	Fe–N(2)	2.071 (2)
S(1)–C(1)	1.610 (2)	C(1)–N(2)	1.165 (3)
N(1)–C(3)	1.384 (3)	N(1)–C(2b)	1.332 (2)
C(2)–C(3)	1.384 (3)		
Angles			
N(1)–Fe–N(1c)	88.4 (1)	N(1)–Fe–N(1a)	180.0 (1)
N(1)–Fe–N(1d)	91.6 (1)	N(1)–Fe–N(2)	89.3 (1)
N(1)–Fe–N(2a)	90.7 (1)	N(2)–Fe–N(2a)	180.0 (1)
Fe–N(1)–C(3)	119.6 (1)	Fe–N(1)–C(2b)	124.9 (1)
C(3)–N(1)–C(2b)	115.4 (2)	N(1)–C(3)–C(2)	121.9 (1)
C(3)–C(2)–N(1b)	122.7 (2)	Fe–N(2)–C(1)	156.9 (3)
S(1)–C(1)–N(2)	178.3 (3)		

[a] Symmetry code: (a) $-x, -y, -z$; (b) ${}^1/_2 - x, {}^1/_2 - y, -z$; (c) $-x, y, -z$; (d) $x, -y, z$.

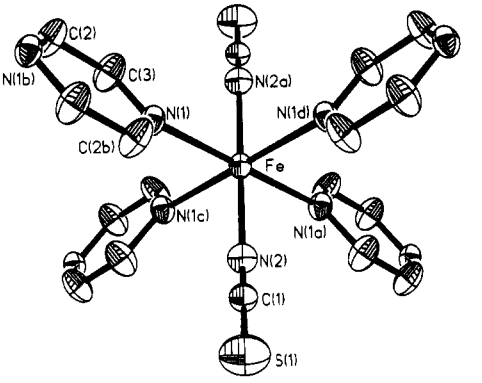

Figure 1. ORTEP view of the coordination sphere of iron(II), showing the atom numbering and thermal motion ellipsoids (30%). The hydrogen atoms are not represented for clarity.

Results and Discussion

Description and Structure. The structure is made up of parallel sheets each consisting of an infinite square array of iron atoms bridged by bismonodentate pyrazine groups, with monodentate N-bound thiocyanato anions above and below the poly($Fe(pyz)_2$) plane achieving the pseudooctahedral configuration around each iron atom (Figures 1 and 2). The sheets alternate so that the iron atoms in one sheet lie vertically above and below the centers of the squares formed by the iron atoms of adjacent sheets.

The coordination geometry about each iron(II) ion is that of a tetragonally compressed octahedron: the basal plane is defined by four pyrazine-N atoms, and the axial positions are occupied

(8) Golstein, M.; Taylor, F. B.; Unsworth, W. D. *J. Chem. Soc., Dalton Trans.* **1972**, 418.
(9) (a) Inoue, M.; Kubo, M. *Coord. Chem. Rev.* **1976**, *21*, 1. (b) González, D.; Bartolomé, J.; Navarro, R.; Greidanus, F.; de Jongh, L. J. *J. Phys. Colloq.* **1978**, *39*, 762. (c) Carlin, R. L.; Carnegie, D. W.; Bartolomé, J.; González, D.; Floria, L. M. *Phys. Rev. B* **1985**, *32*, 7476.
(10) (a) Haynes, J. S.; Sams, J. R.; Thompson, R. C. *Inorg. Chem.* **1986**, 25, 3740 and references therein. (b) Haynes, J. C.; Kostikas, A.; Sams, J. R.; Simopoulos, A.; Thompson, R. C. *Inorg. Chem.* **1987**, *26*, 2630.
(11) Earnshaw, A. *Introduction to Magnetochemistry*; Academic Press: London and New York, 1968.
(12) SHELXTL PLUS, Version 3.4. Siemens Analytical X-Ray Instruments Inc., Madison, WI, 1989.
(13) Nardelli, M. *Comput. Chem.* **1983**, *7*, 95.
(14) Supplementary material.

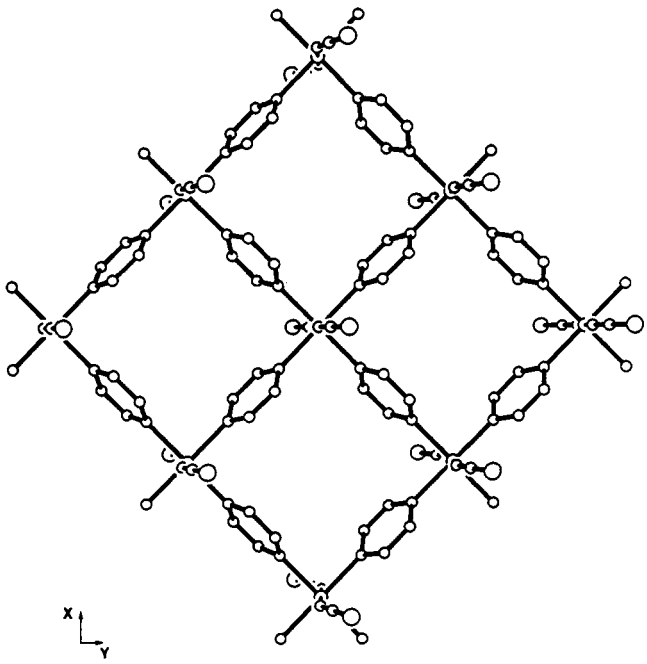

Figure 2. View of a sheet of $[Fe(pyz)_2(NCS)_2]_n$ along the plane perpendicular to the xy one.

by two thiocyanate-N atoms. The Fe, N(1), N(1a), N(1c), and N(1d) atoms lie exactly in a plane. The four equatorial distances are equal (2.246 (2) Å) and somewhat longer than the axial ones (2.071 (2) Å). The Fe–N(pyrazine) bond length is longer than the reported ones in the related $Co(pyz)_2Cl_2$ (2.18 (1) Å)[3a] and $Cu(pyz)_2(ClO_4)_2$ (2.062 (3) Å).[3c] Only small deviations from ideal values are observed in the bond angles of the coordination polyhedron of iron(II) (maximum 1.6°).

The pyrazine rings are found to be planar within experimental errors. Bond distances and angles of the ring compare well with those reported for other pyrazine-containing compounds.[3,4,15] The pyrazine rings are canted relative to the $Fe-N_4$ equatorial plane, the dihedral angle between both planes being 64°. The distance between two adjacent sheets is 6.278 (1) Å, the shortest intersheet contacts being 4.817 (2) Å (sulfur–iron). The iron–iron distance through pyrazine is 7.297 (1) Å, whereas the shortest iron–iron distance between sheets is 7.155 (2) Å.

Whereas the terminal thiocyanato groups are quasi-linear (S(1)–C(1)–N(2) = 178.3 (3)°), the Fe–N–C(S) linkages are bent (Fe–N(2)–C(1) = 156.9 (3)°). These structural features have been observed in other complexes where the terminal NCS groups are N-bonded.[16]

Magnetic Properties. As reported previously,[10b,17] the compound $[Fe(pyz)_2(NCS)_2]_n$ exhibits a magnetic susceptibility vs temperature curve indicative of an antiferromagnetic exchange interaction throughout the temperature range studied (Figure 3). The curve has a relatively sharp maximum at 8.5 K. According to the crystal structure of $[Fe(pyz)_2(NCS)_2]_n$ we have analyzed its susceptibility data through Line's high-temperature series expansion for a two-dimensional square-planar antiferromagnet in the Heisenberg limit[18] with the exchange Hamiltonian defined as $H = -\sum_{i,j} JS_iS_j$. A least-squares procedure that minimizes the function R, $R = \sum(\chi_M^{obsd} - \chi_M^{calcd})^2 / \sum(\chi_M^{obsd})^2$, leads to the J and g values. The best fit through all experimental data was obtained with $J = -1.02$ cm^{-1} and $g = 2.36$ ($R = 1.47 \times 10^{-3}$).

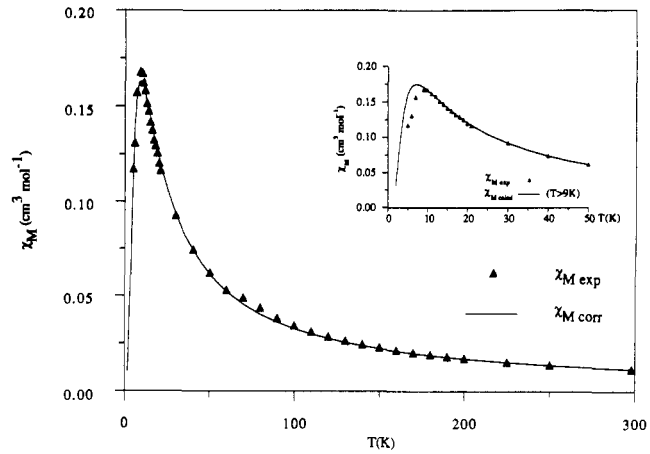

Figure 3. Thermal variation of the magnetic susceptibility per mole of iron (χ_M) of $[Fe(pyz)_2(NCS)_2]_n$. The solid line represents the best fit to data (upper curve corresponds to the fit without mean-field correction, taking only into account high-temperature points ($T > 9$ K) and lower curve corresponds to the fit considering all experimental data and interlayer interactions).

The computed curve does not give a satisfactory match to the experimental data in the vicinity of the maximun of χ_M, as observed by others authors.[10b] Such a discrepancy has been attributed to inadequacies in the model as applied to an $S = 2$ manifold (the model neglects zero-field-splitting effects as well as any extended three-dimensional order). Calculations that were done by using the high-temperature data only ($T > 9$ K) lead to similar J and g values (−0.80 cm^{-1} and 2.48, respectively) but with a much better fit ($R = 8 \times 10^{-5}$, upper curve in Figure 3). The fact that the data on the low-temperature side of the maximum are well below the theoretical curve suggests that significant interlayer interactions are operative. In order to take them into account, we have incorporated a standard mean-field correction of the form $\chi_{corr} = \chi_M/[1 - (2z'J'/Ng^2\beta^2)\chi_M]$, where $z'J'$ is the interlayer interaction. Least-square fitting of all experimental points leads to J, $z'J'$, and g values of −1.1 cm^{-1}, −1 cm^{-1}, and 2.12, respectively, with an agreement factor $R = 6 \times 10^{-4}$ (solid line of the lower curve in Figure 3). This fit is not as good as the preceding one, but it is better than the first one reflecting that interlayer interaction is not negligible. Magnetic anisotropy studies on single crystals are needed to investigate thoroughly the 2D to 3D magnetic ordering.

A comparison of the exchange coupling in $[Fe(pyz)_2(NCS)_2]_n$ and $[Cu(pyz)_2(ClO_4)_2]_n$[3c] is in order in the light of their structural similarities: both structures consist of sheets of bivalent ions bridged by bis-monodentate pyrazine groups, with nearly identical dihedral angles between the plane of each pyrazine ligand and the sheet in which it is located. Two weakly coordinated perchlorate anions achieve a tetragonally elongated octahedron around Cu(II), whereas two coordinated thiocyanate groups lead to a tetragonally compressed octahedron around Fe(II). When the number of unpaired electrons on each magnetic center is taken into account (one for Cu(II) and four for Fe(II)), and the $n^2|J|$ values[19] are compared, a somewhat larger value is obtained for the copper(II) compound (5.3 and 4 cm^{-1} for Cu(II) and Fe(II), respectively). The higher efficiency of bridging pyrazine to transmit electronic effects in the copper(II) complex with respect to the iron(II) compound can be understood as follows: the interaction of the metal orbitals that contain the unpaired electron through the pyrazine bridge depends on (i) the overlap between the 3d orbitals and the bridge symmetry-adapted molecular orbitals and also on (ii) the energy difference between these orbitals. From these two factors a smaller interaction is predicted when Cu(II) is substituted for Fe(II). The Fe(II)–N(pyrazine) bond distance is longer than the corresponding one involving Cu(II),

(15) Beattie, J. K.; Hush, N. S.; Taylor, P. R.; Raston, C. L.; White, A. H. *J. Chem Soc., Dalton Trans.* **1977**, 1121.
(16) (a) Real, J. A.; Zarembowitch, J.; Kahn, O.; Solans, X. *Inorg. Chem.* **1987**, *26*, 2939. (b) Jide, X.; Shisheng, N.; Yujuan, L. *Inorg. Chem.* **1988**, *27*, 4651. (c) Antolini, L.; Fabretti, A. C.; Gatteschi, D.; Giusti, A.; Sessoli, R. *Inorg. Chem.* **1990**, *29*, 143. (d) Gallois, B.; Real, J. A.; Hauw, C.; Zarembowitch, J. *Inorg. Chem.* **1990**, *29*, 1152.
(17) Figgis, B. N.; Lewis, J.; Mabbs, F. E.; Webb, G. A. *J. Chem. Soc. A* **1967**, 442.
(18) Lines, M. E. *J. Phys. Chem. Solids* **1970**, *31*, 101.
(19) (a) Gired, J. J.; Charlot, M. F.; Kahn, O. *Mol. Phys.* **1977**, *34*, 1063. (b) Charlot, M. F.; Gired, J. J.; Kahn, O. *Phys. Status Solidi B* **1978**, *86*, 497.

and the energies of the Cu(II) d orbitals are the lowest of the bivalent ion complexes in the first transition series. So, the overlap between the single-occupied $3d_{x^2-y^2}$ orbitals and the symmetry-adapted σ orbital of pyrazine is smaller for Fe(II) than for Cu(II) leading to a weaker antiferromagnetic coupling. Although a π pathway involving likely the $3d_{xz}$ and $3d_{yz}$ magnetic orbitals of Fe(II) would reinforce the antiferromagnetic coupling in this compound, the existence of ferromagnetic terms[19] for a multielectron center such as Fe(II) counterbalances this additional antiferromagnetic contribution and leads to the above mentioned trend of J values.

To conclude, the use of slow-diffusion techniques enabled us to grow single crystals of the insoluble polymeric $[Fe(pyz)_2(NCS)_2]_n$ compound. Its crystal structure was solved, and its magnetic properties were reinvestigated and compared to the ones of related systems in the light of available structural data. More efforts should be devoted to obtain single crystals of such nice low-dimensional systems in order to establish useful magneto–structural correlations.

Acknowledgment. We are very grateful for the funding of this research by the Dirección General de Investigación Científica y Técnica (Spain) (Proyecto PB88–0490) and the Italian Ministery of Education. We are indebted to Dr. S. Flandrois for his help with magnetic measurements.

Supplementary Material Available: Tables of crystallographic and structure refinement data (Table S1), thermal parameters (Table S2), and hydrogen coordinates (Tables S3) and a projection of the structure of $[Fe(pyz)_2(NCS)_2]_n$ along the diagonal of the xy plane (Figure S1) (4 pages); a listing of observed and calculated structure factors (Table S4) (3 pages). Ordering information is given on any current masthead page.

Additions and Corrections

1990, Volume 29

Ronald R. Ruminski* and Jaqueline L. Kiplinger: Synthesis and Characterization of Cyanoiron(II) Complexes Bound to the Bridging Ligand Tetrakis(2-pyridyl)-1,4-diazine (tpd).

Page 4583. In Table III, the ion $[Ru(tpd)_2]^{2+}$ should replace the ion $[Ru(tpy)(tpd)]^{2+}$, and $H_{4'}$ for $[Fe(CN)_3(tpd)]^-$ is at 7.58 ppm.

Page 4584. Beginning at the sixth sentence of the first complete paragraph, the text should read as follows: It is of interest to note that for the $[(Fe(CN)_3)_2(tpd)]^{2-}$ ion, the $H_{6'}$ doublet is shifted downfield with respect to the $H_{4'}$ and $H_{5'}$ triplets, in contrast with the case for the previously reported $[(Ru(tpy))_2(tpd)]^{4+}$ ion, where $H_{6'}$ was reported further upfield from the $H_{4'}$ triplet. The comparative upfield shift observed for $H_{6'}$ in the bimetallic $[(Ru(tpy))_2(tpd)]^{4+}$ ion is attributed to that proton being held in a strongly shielding position above the plane of the orthogonal tpy ligand. The relative downfield position of $H_{6'}$ in the bimetallic Fe complex is due to the proton being held coplanar and being in the deshielding region of the adjacent rings. The monometallic complex displays four sets of doublets and four sets of triplets for uncoordinated and coordinated rings. Doublets at 8.82, 8.74, 8.04, and 6.98 ppm are tentatively assigned to H_6, H_3, $H_{6'}$, and $H_{3'}$, respectively. As reported for the monometallic ruthenium complex,[23] the uncoordinated pyridine ring presumably rotates out of plane, resulting in an upfield shift of the coordinated $H_{3'}$ proton. The position of $H_{3'}$ in $[Fe(CN)_3(tpd)]^-$ at 6.98 ppm is consistent with the previous rationale.—Ronald R. Ruminski